Monitoring Biological Surfaces for *Salmonella enterica* Resistance in a Fluidic Channel

Lindsay Hoey

Advisor: Professor Christopher R. Lambert

April 2024

Abstract

Salmonella enterica poses a significant global public health risk due to its ability to cause serious disease and form biofilms that protect the bacteria and facilitate their spread. These infections are difficult to treat and cost nearly $4 billion annually in the U.S. alone. Biofilm formation begins with the attachment of bacteria to a surface, commonly inert surfaces like medical or food preparation devices. The growing prevalence of antibiotic-resistant bacteria, combined with the ineffectiveness of systemic antibiotics after biofilm formation, highlights the urgent need for strategies to prevent initial bacterial attachment. Utilizing an innovative flow-through channel to investigate adhesion as a function of surface chemistry, it was found that hydrophobic surfaces were the most effective at reducing *S. enterica* attachment. Surfaces were also derivatized with P22, a bacteriophage for *S. enterica*. These surfaces captured the most bacteria, but it was also found that the phage were still active following attachment and therefore bactericidal. The ultimate outcome of this work will be the fabrication of surfaces that inhibit *S. enterica* biofilm formation, with applications in healthcare and food safety. The technology also suggests a method to improve the sensitivity of bacterial detection.

Acknowledgements

Table of Contents

1. Introduction

Salmonella enterica is known for its propensity to form dense biofilms on surfaces, posing significant health risks in medical and food safety environments. Biofilms facilitate the proliferation of bacteria and elevate the risk of infections from pathogens. Given that biofilm formation initiates with the attachment of bacteria to a surface, employing technologies that inhibit bacterial adhesion is crucial for reducing biofilm development. The work presented tested three surface modifications (glutaraldehyde, a fluorinated silane, and P22 bacteriophage) designed to resist bacterial colonization under dynamic flow conditions. Bacterial load was quantitatively assessed on each modified surface to identify the most effective treatments for minimizing bacterial adhesion and subsequent biofilm formation.

1.1 *Salmonella enterica*

Salmonella enterica, a gram-negative, facultative anaerobic bacterium, presents significant public health risks globally (Bhunia, 2018; Eng, 2015). Its ability to survive at low pH and thrive in temperatures ranging from 5 – 45°C, and optimally at 35 – 37°C, makes S. enterica adaptable to a wide range of environments, contributing to its prevalence as a major foodborne pathogen (Bhunia, 2018). According to the U.S. Center for Disease Control and Prevention approximately 1 million Americans contract Salmonella infections, annually (Hoffmann, 2015). While most healthy individuals experience transient symptoms, severe cases can lead to hospitalization or even death – of the 1 million Americans, 19,000 are admitted to hospitals, and 380 infections result in death. Medical costs and lost productivity, due to infection, cost the US upwards of $3.7 billion, making S. enterica the foodborne pathogen with the most economic burden. The primary infection vectors for S. enterica are food animals such as swine, poultry, and cattle, with transmission occurring predominantly by the fecal – oral route through contaminated meat, poultry, eggs, and produce (Eng, 2015; Ly, 2007; Pui, 2011).

At the molecular level, S. enterica employs a sophisticated mechanism to invade host cells. Upon ingestion, the bacteria forms colonies within the intestinal epithelium by inducing their own uptake by phagocytosis, facilitated by a complex array of effector proteins delivered into the host cell cytoplasm *via* a Type III secretion system (T3SS) (Galan, 1996; Ohl & Miller, 2001). This action significantly alters the host's actin cytoskeleton, causing extensive membrane protrusions that lead to the engulfment of the bacteria. Furthermore, the T3SS is encoded by *Salmonella*

pathogenicity island-1 (SPI-1) and SPI-2 (Shea *et al.,* 1996). Together, these facilitate a "molecular syringe" mechanism that allows *S. enterica* to insert into the plasma membrane of the host cell (Galan & Wolf-Watz, 2006). These adaptations not only facilitate cellular invasion but also enhance intracellular survival, complicating the treatment of infections.

S. enterica infections involving invasive serotypes pose significant health risks and often require effective antibiotic treatment. However, the rise of antimicrobial resistance in *Salmonella* strains has become a critical global health issue (Chiu *et al.,* 2002). Data from the National Antimicrobial Resistance Monitoring System (NARMS) for 2005-2006 indicates that 84% of clinical non-typhoidal *Salmonella* (NTS) isolates, such as *S. enterica*, exhibited multi-drug resistance (MDR) characteristics (Eng, 2015). Further research indicates that MDR *Salmonella* serotypes are capable of producing hybrid plasmids, with the majority of these plasmids containing gene cassettes that provide these bacteria with resistance to conventional antibiotics (Guerra *et al.,* 2002; Guerra *et al*., 2001).

1.2 Biofilms

According to the National Institutes of Health (USA), biofilms are now recognized as the primary form of bacterial proliferation, responsible for around 80% of all bacterial infections (Steenackers, 2012). These structures are communities of bacteria that attach to surfaces or to each other, enveloped in a self-generated protective matrix of exopolysaccharides (EPS) *(Homoe et al.,* 2009; Steenackers, 2012). This matrix not only acts as a scaffold but also secures vital nutrients close to the bacteria, enhancing their survival (Decho, 2000). As seen in Figure 1, biofilm formation is gradual and begins with the initial adhesion of bacteria to a surface (Bordi, 2011). Over time, as the bacterial concentration on the surface increases, microcolonies form, which can then mature into a fully developed biofilm. Mature biofilms are capable of dispersing new bacteria to neighboring surfaces, continuing the cycle of growth. Notably, *Salmonella* biofilms have been observed on a variety of surfaces such as plastic (Hurrell *et al.,* 2009; Joseph, 2001), rubber (Arnold & Yates, 2009), cement (Joseph, 2001), glass (Prouty & Gunn, 2003), and stainless steel (Giaouris & Nychas, 2006; Joseph, 2001), which are commonly encountered in medical, food processing, and food packaging environments.
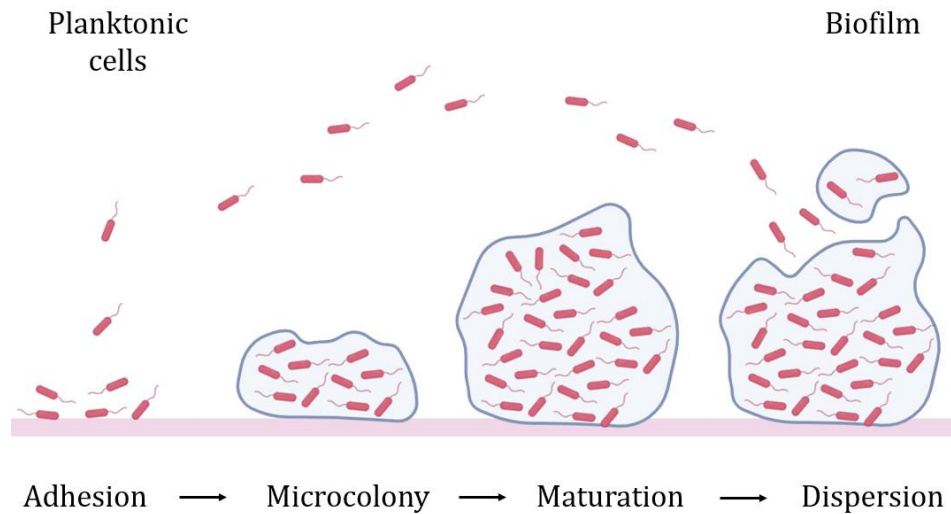
Figure 1. Steps of biofilm formation, beginning with adhesion of bacteria. With increased bacterial number on a surface, microcolonies form and mature into biofilm. Mature biofilms can disperse bacteria and promote further biofilm formation. (Adapted from Bordi, 2011)

The resilience of biofilms is greatly enhanced by their architecture. The matrix facilitates efficient nutrient transport throughout the biofilm, supporting cells that are far from the surface (Bazaka *et al.,* 2012). Simultaneously, it acts as a barrier that inhibits the diffusion of harmful agents such as antibiotics and antibacterial chemicals from reaching the inner layers of the biofilm (Bazaka *et al.,* 2012; Homoe *et al.,* 2009). This protection often causes antibiotics to fail in penetrating the entire biofilm, with the polymeric substances in the matrix slowing down the diffusion rates of these molecules (Homoe *et al.,* 2009). This mechanism significantly reduces the effectiveness of systemic antibiotics typically used for treating infections and diminishes the action of antibacterial agents intended to disrupt these robust bacterial communities.

1.3 Surface Chemistry and Preventing the Landing of Bacteria

Biofilms tend to form on inert surfaces or dead tissue, often colonizing medical and food preparation devices (Costerton *et al.,* 1999), making it critical to prevent infections before they establish. The increasing prevalence of antibiotic-resistant bacteria further complicates the management of infections associated with biomaterials. Systemic antibiotics, traditionally used after biofilm has already formed, frequently deliver suboptimal results and contribute to the spread of antimicrobial resistance (Bazaka *et al.,* 2012). Consequently, there is a heightened need for approaches that prevent initial bacterial attachment and subsequent biofilm formation.

Surface modification of biomaterials emerges as a solution to mitigate pathogenic biofouling and reduce dependence on traditional antibiotics (Bazaka *et al.*, 2012). This method involves chemically treating various substrates, such as metals and non-metals, including biocompatible materials, to alter their properties. Techniques such as oxygenated plasma cleaning enable the precise deposition of coatings that adjust the surface characteristics of these materials (Biederman, 2011). Typically, this process prepares the surface for adding an organic matrix, incorporating functional groups through silane coupling chemistry (Sardella, 2006).

Glutaraldehyde. Glutaraldehyde (Fig. 2), a saturated dialdehyde, is widely utilized as a disinfectant and chemical sterilant due to its robust antimicrobial properties (McGucken & Woodside, 1973; Sehmi *et al.*, 2016). These properties are derived from its capacity to alkylate key biomolecules, including hydroxyl, carbonyl, and amino groups, thereby hindering the synthesis of DNA, RNA, and proteins. Further research has shown that glutaraldehyde can strongly adhere to the outer membrane and block membrane transport in Gram-negative bacteria, further inhibiting these cellular processes (Maillard, 2005).
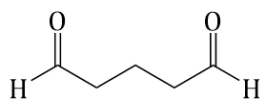
Figure 2. Glutaraldehyde.

Fluorinated Silane. In this study, (tridecafluoro-1,1,2,2-tetrahydrooctyl) trimethoxy silane (Fig. 3), featuring a silane group and a long-fluorinated chain, is utilized to create a hydrophobic surface. Hydrophobic surfaces with low-surface energies are engineered to reduce interactions with biomolecules, effectively preventing strong polar interactions such as hydrogen or ionic bonding (Pistone *et al.*, 2021). This characteristic weakens the adherence of biomolecules and bio-organisms to these surfaces, facilitating their removal through fouling release mechanisms. Moreover, the presence of strong carbon-fluorine bonds in materials like fluorinated silanes imparts chemical stability and resistance to degradation, thereby prolonging the anti-adhesive effects on treated surfaces (O'Hagan, 2008).
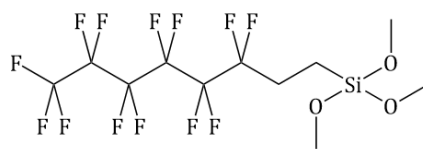
Figure 3. Tridecafluoro-1,1,2,2-tetrahydrooctyl trimethoxy silane.

P22 Bacteriophage. Bacteriophages, also called phages, are viruses that exclusively infect and replicate within bacterial cells (Kasman & Porter, 2024). Phage structures can include "heads," "legs," and "tails" (Fig. 4), and despite these morphological features, phages are non-motile (Wang et al., 2019). The tail of a phage plays roles in host-cell recognition, attachment, cell envelope penetration, and genome ejection. Phages exhibit high species specificity, generally infecting only specific bacterial species or strains – the P22 bacteriophage, which specifically targets *Salmonella enterica* (Vander Byl & Kropinski, 2000), was employed in this study. P22 phage can replicate in two ways: lytic and lysogenic (Kasman & Porter, 2024). In the lytic cycle, the phage hijacks the host's cellular machinery to produce new phages, ultimately causing the host cell to lyse and release progeny phages. In contrast, the lysogenic cycle involves the integration of the phage genome into the host's chromosome or maintenance as an episomal element, replicating passively within the host without causing immediate harm. These integrated viral genomes can revert to the lytic cycle under specific environmental triggers, leading to the destruction of the host cell.
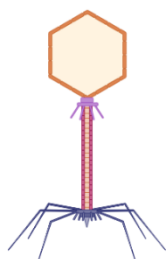
Figure 4. Structure of a bacteriophage, showing the head (orange), tail (pink), and legs (blue).

2. Materials and Methods

Unless otherwise stated, all chemicals for this study were provided by Alfa Aesar (Ward Hill, MA). Phosphate buffered saline (PBS) was made at a pH of 7.4, comprising a solution of 10 mM sodium dihydrogen phosphate, 10 mM sodium hydrogen phosphate, and 140 mM sodium chloride in deionized water. All material needed for the fabrication of PDMS were procured from Gelest (Morrisville, PA).

2.1 Fluidic Channel

A miniature fluidic device (Fig. 5) was crafted using polycarbonate and used a piece of ARflow 93049 waterproof adhesive, from Adhesives Research (Glen Rock, PA) to seal the top surface. The device was used to flow bacteria over derivatized surfaces, and subsequently measure the amount of *Salmonella* adhesion on each surface.
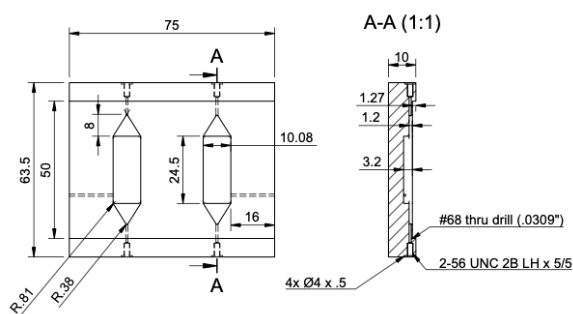
Figure 5. Schematic of polycarbonate fluidic channel, showing sizing and dimensions of the components.

2.2 Fabrication of PDMS

The steps for the fabrication of PDMS were obtained Professor Daniel Schmidt from the University of Massachusetts Lowell (personal communication. 2019). Vinyl-terminated polydimethylsiloxane (VDMS) with a molecular weight of 28,000 (containing 25-35% methylhydrosiloxane), dimethylsiloxane copolymer (HMS), along with a Pt-octanal complex in octanol (2.0-2.5% Pt-complex concentration), were mixed thoroughly using a vortex mixer for 30 seconds. The mixture was poured into an aluminum mold (crafted by Ian Anderson at WPI) designed to fabricate polydimethylsiloxane (PDMS) coupons with dimensions appropriate for incorporation into the fluidic channel, with each coupon receiving 0.43g of the mixture. The mold was then degassed under vacuum for 20 minutes and subsequently heated at 70°C for 20 minutes. The mixing ratio was 3 grams of VDMS to 0.214 grams of HMS and 5 μL of the Pt catalyst.

Additionally, the stiffness of the lab-made PDMS was tested against the stiffness of commercial SYLGUARD 184 silicone elastomer, obtained from Dow (Midland, MI), to determine if the lab-made PDMS was comparable to the commercial PDMS. This was done by casting ~1cm of both types of PDMS in 5-dram vials and comparing stiffness between the two samples using a manual tensiometer built in house.

2.3 Derivatization of Biological Interfaces

Derivatization of the surface was carried out as previously described in fibroblast extracellular matrix and adhesion on microtextured polydimethylsiloxane scaffolds (Stanton, 2015).

Plasma Cleaning. The chamber of an SPI Plasma Prep II was flushed with oxygen gas (O_2) for 5-10 minutes, before the PDMS coupons were placed in the chamber and subjected to vacuum, to achieve a reduced pressure environment. Once the pressure reached a value around 300 atm., the plasma was activated for 15 minutes. The presence of plasma can be seen in the chamber as a blue/white hue.

1% APTMS Surface. 50 µL of 3-aminopropyl trimethoxysilane (APTMS) purchased from Gelest (Morrisville, PA) was diluted in ethanol to achieve a final volume of 5mL, resulting in a 1% APTMS solution. The plasma cleaned PDMS coupons were then submerged in a dish of this solution for one hour to undergo surface modification through silanization. Following derivatization, the coupons were removed from the solution with tweezers, rinsed with ethanol to remove residual APTMS, and dried in a stream of argon gas. Attachment was confirmed *via* contact angle goniometry.

2% Glutaraldehyde Surface. 500 µL of 25% glutaraldehyde was diluted in 5.75 mL of PBS, resulting in a 2% glutaraldehyde solution. The PDMS coupons, derivatized with an amine surface, were submerged in a dish of this solution for one hour to facilitate further derivatization. Following one hour, the coupons were removed from the solution, rinsed with PBS to remove residual glutaraldehyde, and dried in a stream of argon gas. Attachment was confirmed *via* contact angle goniometry.

1% Fluorinated Silane. 50 µL of (tridecafluoro-1,1,2,2-tetrahydrooctyl) trimethoxysilane procured from Gelest (Morrisville, PA) was diluted in ethanol to achieve a final volume of 5mL, resulting in a 1% fluorinated silane solution. The plasma cleaned PDMS coupons were then submerged in a dish of this solution for one hour to undergo surface modification through silanization. Following derivatization, the coupons were removed from the solution with tweezers, rinsed with ethanol to remove residual fluorinated silane, and dried in a stream of argon gas. Attachment was confirmed *via* contact angle goniometry.

P22 Bacteriophage. The phage preparation was completed according to ATCC guidelines by Seyed Hamed Ghavami and kindly gifted for this project. A 1 mL aliquot of P22 bacteriophage obtained from the ATCC (Manassas, VA), frozen in medium at -80℃, was gradually thawed and processed through a 0.22 µm syringe filter. The sample was further diluted with 2 mL of sterile PBS. The coupons derivatized with glutaraldehyde were placed in the phage solution for a minimum of 20 hours to facilitate the attachment of bacteriophage particles. After attachment, the coupons were removed from the solution with tweezers and rinsed with PBS to remove any unbound phages. Attachment was confirmed *via* contact angle goniometry.

2.4 Cell Cultures

The cells used in experimentation were routinely assessed for their optical density at 500 nm (OD_{500}). Cells with an OD_{500} of 0.8 were harvested and used in experimentation.

Wild Type *Salmonella enterica*. A 1 mL aliquot of wild type *S. enterica* cells purchased from ATCC (Manassas, VA), frozen in medium at – 80°C, was gradually thawed. The 1 mL aliquot was then transferred to a 50 mL conical tube, along with 39 mL of nutrient broth from Becton Dickinson (Franklin Lakes, NJ). The tubes were incubated at 37°C, with shaking, to enhance proliferation. To grow fresh cultures, 1 mL of an existing wild type culture (no more than 72 hours old) was inoculated into a fresh 50 mL conical tube, with 39 mL of nutrient broth. These cultures were also placed in an incubator at 37°C, with shaking, to enhance proliferation.

eGFP *Salmonella enterica*. Using genetically engineered *S. enterica* with enhanced GFP (eGFP) and ampicillin resistance (kindly provided by Megahn Barry at WPI Worcester, MA), a 1 mL aliquot of eGFP *S. enterica* cells, stored at -80°C, was gradually thawed. The thawed 1 mL aliquot was then transferred to a 50 mL conical tube, along with 39 mL of nutrient broth and 40 µL of 1000x diluted ampicillin. The tubes were incubated at 37°C, with shaking, to enhance proliferation. To construct

new cultures, 1 mL of an existing eGFP culture (no more than 72 hours old) was inoculated into a fresh 50 mL conical tube, with 39 mL of nutrient broth and 40 µL of 1000x diluted ampicillin. These cultures were also placed in an incubator at 37°C, while shaking, to enhance proliferation.

2.5 Enumerating Bacteria

The procedure for the enumeration of bacteria was derived from (Pakpour, 2021) and is described here briefly.

Wild Type *S. enterica*. Serial dilutions of wild type cells (OD$_{500}$: 0.8, +/- 0.1) in PBS were made. 100 µL of 10^{-5}, 10^{-6}, and 10^{-7} dilutions were evenly spread across 3.7% (37 g LB Agar in 1 L of deionized water) LB agar plates with a sterilized glass spreader. LB agar was obtained from Becton Dickinson (Franklin Lakes, NJ). The plates were wrapped in Parafilm, and the liquid was left to absorb for 10 minutes before inverting and being placed in an incubator at 37°C for 24 hours. The plates showing 30 – 300 colonies were counted. The total bacterial concentration (cells/mL) was calculated by dividing the number of colonies by the amount plated (in mL) then dividing by the dilution factor.

eGFP *S. enterica*. Serial dilutions of eGFP cells (OD$_{500}$: 0.8, +/- 0.1) in PBS were made. 100 µL of 10^{-2}, 10^{-3}, and 10^{-4} dilutions were evenly spread across 3.7% LB agar plates that include ampicillin, with a glass spreader. The plates were wrapped in Parafilm, and the liquid was left to absorb for 10 minutes before inverting and being placed in an incubator at 37°C for 24 hours. Once colonies were visible, the plates were placed under UV light to ensure the cells were fluorescent. The plates showing 30 – 300 colonies were counted. The total bacterial concentration (cells/mL) was calculated by dividing the number of colonies by the amount plated (in mL) then dividing by the dilution factor.

2.6 P22 Phage Interaction with *S. enterica*

Activity of Phage on PDMS. To determine whether the phage was still active upon attachment to the PDMS a flow experiment was conducted. Using PDMS that was derivatized with a phage surface and placed in the fluidic channel, 10mL of 10x diluted wild type bacteria were stained using the *Bac*Light bacterial viability kit, purchased from ThermoFisher (Waltham, MA), and loaded into a syringe. To prevent photobleaching of the fluorescent dye, the experiment was conducted in subdued light. The syringe, mounted on a Chemyx Fusion 101 syringe pump (Stafford, TX), was set

to dispense at a rate of 0.1 mL/min, allowing bacterial cells to flow across the phage modified PDMS surface for 25 minutes. The PDMS was imaged using a Nikon E600 fluorescence microscope (Melville, NY), with a 20 X water immersion lens (NA=0.5), for the duration of the experiment and images were taken at 2-minute intervals and processed using Nikon Elements 5.0 software. In the staining assay, SYTO-9 stains live cells green, whereas propidium iodide stains dead cells red. The ratio of live to dead cells on the phage surface was analyzed to determine the bacteriophage's efficacy on PDMS. This process was repeated on an amine surface, as a control.

Spot Test. 150 μL of undiluted eGFP *S. enterica* (OD_{500}: 0.8, +/- 0.1) was spread across a 3.7% LB Agar plate. Once the liquid absorbed into the agar, four quadrants were drawn on the plate. 5 μL of an undiluted P22 bacteriophage sample was spotted in three of the four quadrants. The fourth quadrant was left unspotted as a control. The plate was inverted and placed in an incubator at 37°C for 24 hours. To image, the plates were viewed under a Leica EZ4 stereo microscope. Images were taken at the points of spotting and compared to the control quadrant, to assess the phage's impact on the eGFP colonies.

2.7 Imaging Phage Using SEM

To visualize the attachment of phage on a PDMS surface, a Schottky emission gum SEM model JEOL 7000F (Peabody, MA) was used for scanning electron microscopy. A PDMS coupon modified with phage was attached to a glass slide using double sided tape. The glass slide was coated in Pd to make the surface of the phage conductive. After it was coated, the glass slide was taped on to the specimen holder using copper tape before being placed into the vacuum chamber of the SEM. The vacuum was turned on until a pressure of 10^{-5} Pa was reached. Once this pressure was reached, the samples were moved to the imaging chamber, where an image was captured at 70,000 X.

2.8 Cell Flow in Fluidic Channel

An apparatus was constructed to allow the flow of cells over a derivatized surface (Fig. 6). A 100 mL syringe, loaded with 80mL of eGFP *S. enterica* and equipped with a magnetic stir bar, was mounted on a syringe pump. The pump was calibrated to administer the cells at a flow rate of 0.05 mL/min. To maintain the cells at a low temperature and slow growth, the syringe was encased in ice throughout the experiment. A tube connected to the syringe *via* an 18G needle, was coiled within a beaker with water maintained at 37°C to stimulate physiological conditions and attached

the ingoing end of the fluidic channel. A coupon of derivatized PDMS was placed inside the channel (shown in red in Fig.6), and a piece of ARflow 960339 waterproof adhesive was placed over top. Another tube was attached to the outgoing end of the channel and the tube was directed into a beaker of bleach. To initiate the experiment, the magnetic stir plate was turned on to ensure constant mixing of the cells, air bubbles were pushed through the channel, and the syringe pump was started. This ran for 48 hours, while cells and ice were replaced as needed. This experiment was repeated for PDMS surfaces derivatized with APTMS, glutaraldehyde, fluorinated silane, and P22 phage.
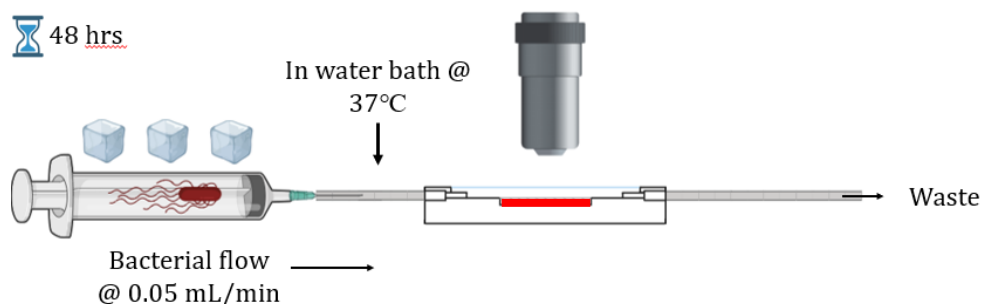
Figure 6. Apparatus used to flow bacteria over the surface of surface modified PDMS.

2.9 Imaging Bacterial Adhesion

Upon conclusion of the 48hr flow experiment, the channel containing the derivatized PDMS was placed under a Nikon E600 fluorescence microscope. Beginning at the end where flow originated from, seven images were taken using the Nikon Elements 5.0 software, at different locations mapped in Figure 7, to visualize and quantify bacterial adhesion to each surface. These seven locations were the same for each derivatization. Each image was processed in ImageJ, before each bacterium was counted using a MATLAB code (Appendix A) and the amount in each image was recorded. The MATLAB excluded based on size (outside 1 – 100 pixels) and shape. Utilization of the eGFP engineered *S. enterica* allowed for imaging of the cells without prior staining.
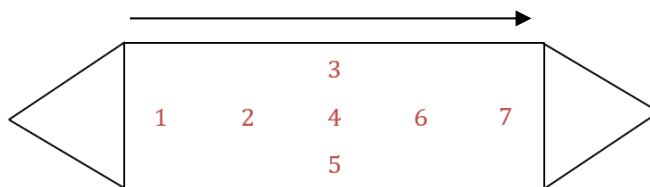
Figure 7. Map of where each of the seven images were taken on the derivatized PDMS, in the fluidic channel. The left side represents where the flow originates, and the right side represents where the flow exits.

3. Results and Discussion

The experiments used in this study demonstrate methods to quantify the number of bacteria adhered to a surface. The following results show that more the hydrophobic surface, the fluorinated silane, was the most effective at reducing bacterial adhesion. Paradoxically, the phage had the highest rate of bacterial landing, but since the phage is still active while on the surface, it proved to be bactericidal. Both surfaces show potential to be effective inhibitors of biofilm, due to their ability to prevent bacterial landing or kill bacteria upon attachment. It is important to note that the amine surface, derivatized from APTMS, was used as a control surface. It is difficult to have clean PDMS present the same contact angle once it has been fabricated and therefore the amine surface was used as a more reliable control surface.

3.1 Stiffness of PDMS

When comparing the tensiometer data of the lab-made PDMS to the commercial PDMS (Fig. 8), the lab-made PDMS is roughly 2/3 of the stiffness of commercial PDMS. To compare our experiments more accurately with published work, future work will be carried out using PDMS that matches the stiffness of the commercial sample more closely.
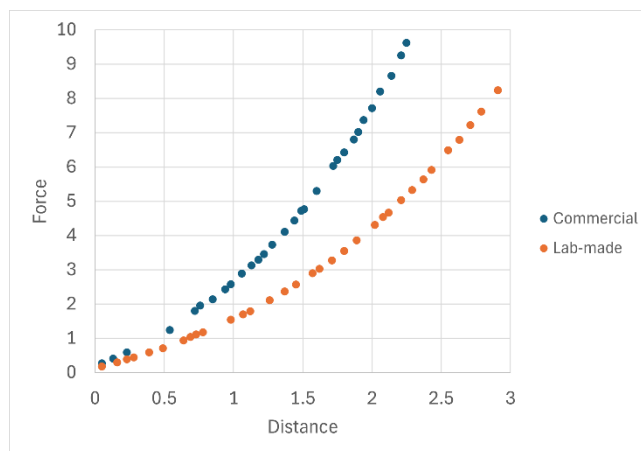
Figure 8. Graph comparing stiffness of lab-made (orange) and commercial (blue) PDMS. The commercial PDMS is slightly stiffer than that of the lab-made PDMS.

3.2 Derivatization

Success of functional group attachment was determined *via* contact angle. Contact angle measures the angle of the edges of a droplet of water on a surface. Any change in contact angle is attributed to a change in surface chemistry, and the more hydrophobic a surface, the larger the contact angle will be. The observed contact angles for O_2 plasma treated PDMS, amine, glutaraldehyde, fluorinated silane, and phage treatment were 27.5°, 0°, 28.5°, 75.0°, and 55.6°, respectively. For each step in derivatization, there is a notable change in contact angle, confirming a change in surface chemistry. The fluorinated silane has the highest contact angle, as expected, since it is the most hydrophobic surface.

3.3 Enumeration of Bacteria and Imaging of P22 Phage

Enumeration of Bacteria. Wild type *S. enterica* plated at a dilution of 10^{-7} and OD_{500} of 0.8 contained 2×10^8 CFU/mL. The eGFP *S. enterica* was plated at a dilution of 10^{-4} and an OD_{500} of 0.7 contained 2.19×10^7 CFU/mL. Figures 9a and 9b show the difference between wild type and eGFP *S. enterica*. It was demonstrated that the bacteria were in log phase when they had an OD_{500} 0.8 +/ 0.1 measured in a 1cm cuvette.

a.
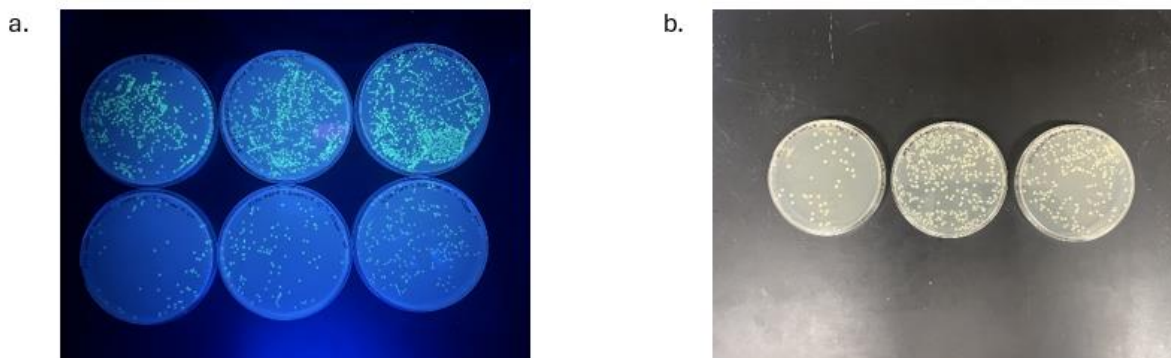
Figure 9. Visual comparison of wild type and eGFP *S. enterica*. a.) eGFP *S. enterica* colonies on LB plate, expressing elevated fluorescence. b.) Wild type *S. enterica* colonies on LB plate, expressing no fluorescence.

Imaging of P22 Phage. Phage heads were visualized using SEM. In Figure 10, each protrusion or bump can be associated with a phage head since they are roughly 60 nm in diameter. The image shows a high density of phage attached to the surface, not only further confirming the attachment of the phage to the surface, but also allowing for increased bacterial entrapment. Enumeration of phage would be beneficial, but conducted experiments proved to be unsuccessful. Determination of the amount of phage/mL could allow for a more accurate determination of the amount of phage on the surface.
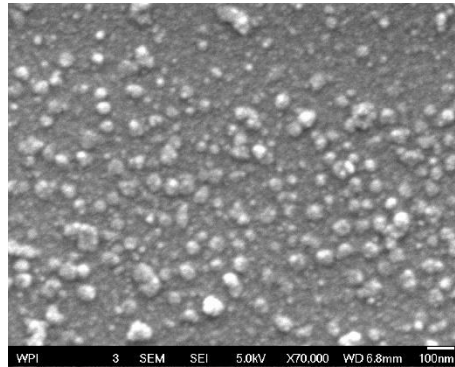
Figure 10. SEM image of P22 bacteriophage attached to the surface of PDMS. P22 phage heads are ~60 nm in diameter, using the scale the protrusions around 60 nm are phage heads. This confirms the attachment of phage to the surface, and a higher concentration of phage can lead to higher trapping of bacteria on the surface.

3.4 P22 Phage interaction with *S. enterica*

Activity of Phage on PDMS. Since the P22 phage will kill the bacteria after entrapment, using the *Bac*Light stain, these cells will fluoresce red under the Nikon E600 fluorescence microscope. If there are greater numbers of red fluorescing cells over time compared with a control culture, this confirms the phage is still active following attachment to PDMS. Figures 11a-c show the relative amount of dead bacteria on the surface of amine derivatized PDMS, at 0, 10, and 25 minutes. Figures 11d-f show the relative amount of dead bacteria on the surface of phage derivatized PDMS, at 0, 10, and 25 minutes. The phage surface has a greater increase of dead bacteria on the surface, when compared to the control surface, showing its maintained activity. However, when processing the images, the dark spots seen in the images threw off the threshold. Due to this, the mages were unable to show an accurate representation of bacteria on the surface using a threshold. Rather, the images were inverted to better see the bacteria – small, round, dark gray/black spots can be closely correlated with *S. enterica* on the surface. The larger, black particles were excluded.
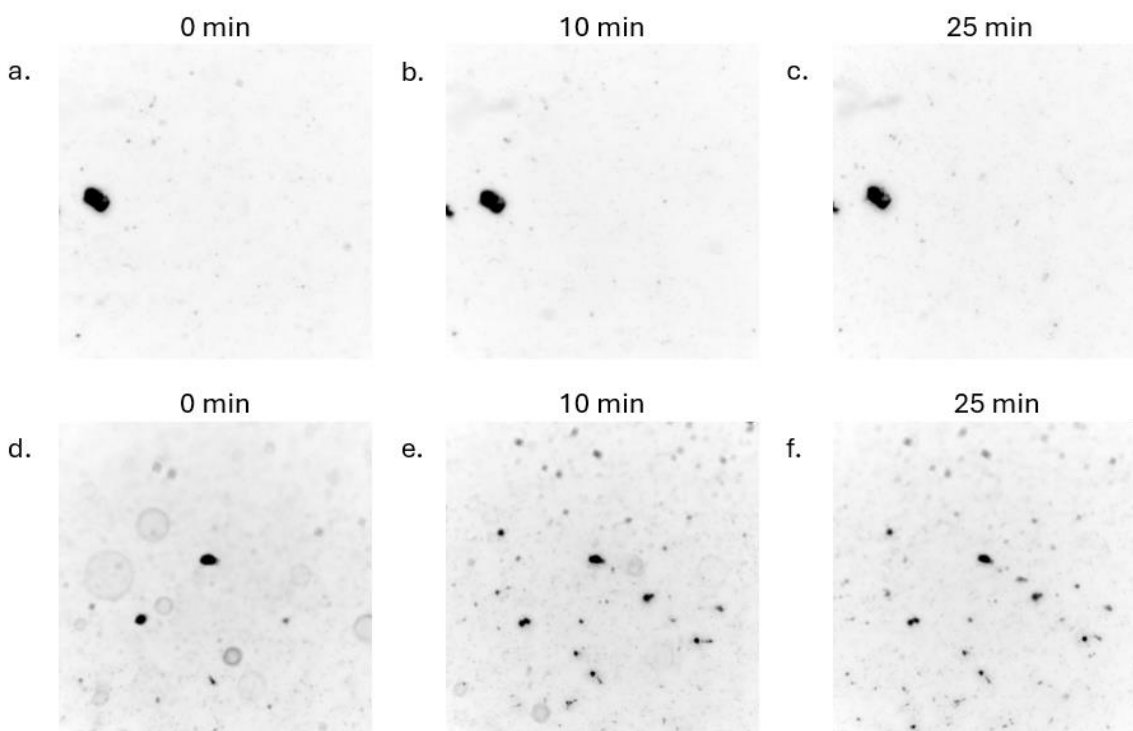
Figure 11. Activity of phage on modified PDMS surface over 25 minutes. a) Amine surface at t = 0; b) amine surface at t = 10; c) amine surface at t = 25; d) phage surface at t = 0; e) phage surface at t = 10; f) phage surface at t = 25. The phage surfaces show a greater increase in bacteria on the surface over time.

Spot Test. After ensuring the phage was active on the surface, and interacted with the wild type *S. enterica*, P22 phage interaction with eGFP *S. enterica* was assessed. The spot test conducted compared three spots of phage on a lawn of bacteria, to an unspotted region of the lawn. Figures 12a – d show the result of the spotting imaged with a Leica EZ4 stereo microscope. The control shown in Figure 12a shows a denser lawn of bacteria on the plate, compared to Figures 12b – d, which show more sporadic colonies of bacteria. The decreased number of bacteria on the surface of the plate correlates to a successful interaction of the eGFP cells with the P22 phage, since the phage will prevent the bacteria from proliferating upon interaction.
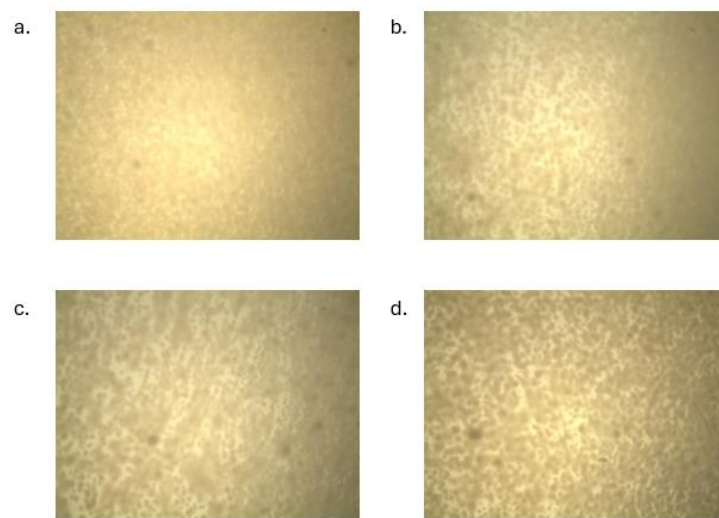
Figure 12. P22 phage interaction with eGFP *S. enterica*. a) Control area on plate, with phage drop; b) Spot one with 5 µL of P22 phage dropped on the surface; c) Spot two with 5 µL of P22 phage dropped on the surface; d) Spot three with 5 µL of P22 phage dropped on the surface.

3.5 *S. enterica* Resistance Determined by Flow on Biological Surfaces

There was difficulty in growing and visualizing *S. enterica* biofilm in this study. Given that *Salmonella enterica* biofilm has a higher tendency to for under stress (decreased nutrients and change in pH or temperature) (Lories *et al.*, 2020), experiments altering these conditions were conducted, but even under stress, biofilm formation was not apparent. These results do not show the capacity of each surface to resist biofilm, but rather the potential of each surface to inhibit biofilm formation, by reducing the number of bacteria that adhere. Additionally, these surfaces were not tested to quantify the ratio of dead bacteria to those that adhered to the surface. Further research can be done to determine if these surfaces not only resist bacteria but prove to be bactericidal. It is expected that the amine surface will not be bactericidal, but a glutaraldehyde one might.

Amine. The PDMS surface treated with 1% APTMS, served as the control. Figures 13a – g show the bacterial count from seven different locations on the surface (mapped in Fig. 6). There was a total of 417 bacteria, with the most bacteria in one spot being 167 (Fig. 13g). This shows a moderately high level of bacterial adhesion, which can contribute to a higher likelihood of biofilm development.
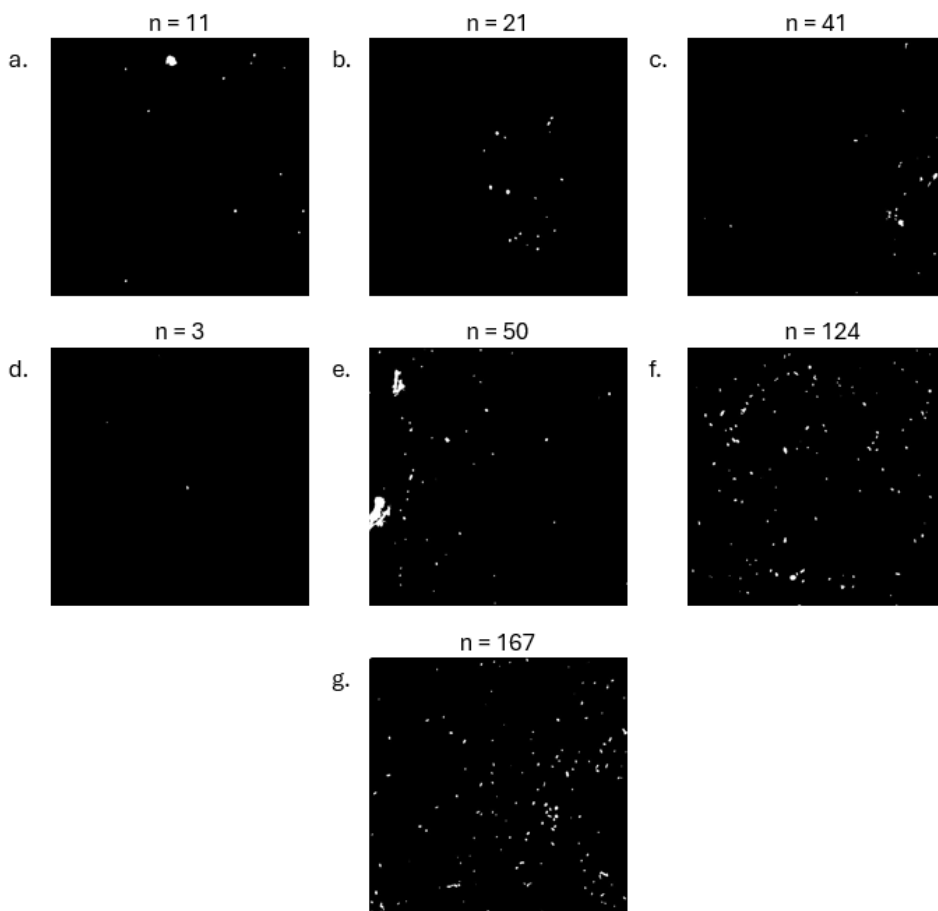
Figure 13. Microscope images of *S. enterica* on the surface of APTMS modified PDMS, where n = number of bacteria. a) spot one showing 11 bacteria; b) spot two showing 21 bacteria; c) spot three showing 41 bacteria d) spot four showing 3 bacteria; e) spot five showing 50 bacteria; f) spot six showing 124 bacteria; g) spot seven showing 167 bacteria. The MATLAB code in Appendix A was used to exclude particles based on size and shape.

Glutaraldehyde. On the surface of the PDMS treated with 2% glutaraldehyde, there was a significant increase in bacterial adhesion, compared to the control. In Figures 14a – g, there are a total of 771 bacteria, with the most bacteria in one spot being 244 (Fig. 14c). This increase is likely due to glutaraldehyde's ability to strongly bind the membrane of Gram-negative bacteria. Due to this, it will be beneficial to determine if glutaraldehyde exhibits bactericidal effects on the attached bacteria. If bactericidal activity is observed, this surface shows promise to inhibit biofilm formation by inhibiting proliferation and activity of the *S. enterica*. In processing microscope images the relative intensity of the overall image is a critical factor in counting bacteria using the MABLAB code script described earlier. It became apparent, that particularly in the images acquired on the glutaraldehyde surface, the numbers of bacteria were actually higher than that determined using the script. This means in fact that, as might be expected, glutaraldehyde traps more bacteria than the control surfaces. This also led us to recount all of our images and to the best of our knowledge the counts are accurate as reported to within an error of approximately 20%. Future work is still needed to determine the potential bactericidal activity of the glutaraldehyde surface.
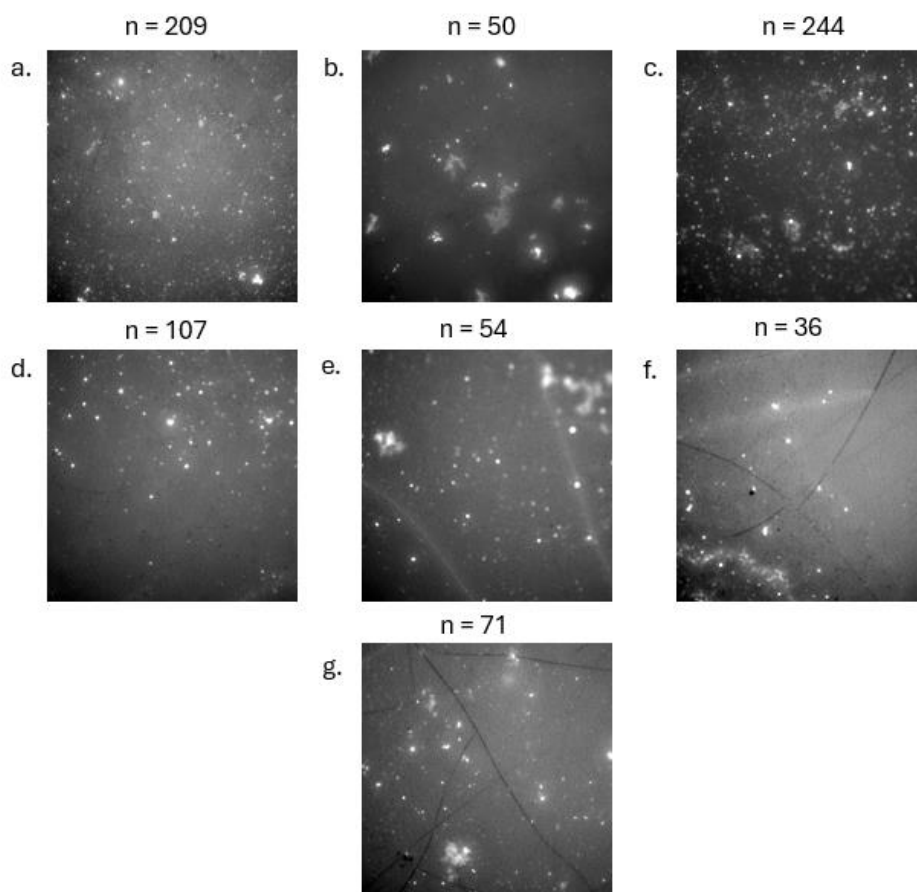
Figure 14. Microscope images of *S. enterica* on the surface of glutaraldehyde modified PDMS, where n = number of bacteria. a) spot one showing 209 bacteria; b) spot two showing 50 bacteria; c) spot three showing 244 bacteria; d) spot four showing 107 bacteria; e) spot five showing 54 bacteria; f) spot six showing 36 bacteria; g) spot seven showing 71 bacteria. The MATLAB code in Appendix A was used to exclude particles based on size and shape.

Fluorinated Silane. The PDMS surface treated with1% (tridecafluoro-1,1,2,2-tetrahydrooctyl) trimethoxy silane, showed to be the most hydrophobic. In Figures 15a – g, there was a significant decrease in the adhesion of bacteria, compared to the amine surface. There was a total of 119 bacteria, with the most bacteria in spot being 30 (Fig 15d). Since this surface has been shown to be the most effective for bacterial resistance, it has the highest potential to inhibit biofilm formation.
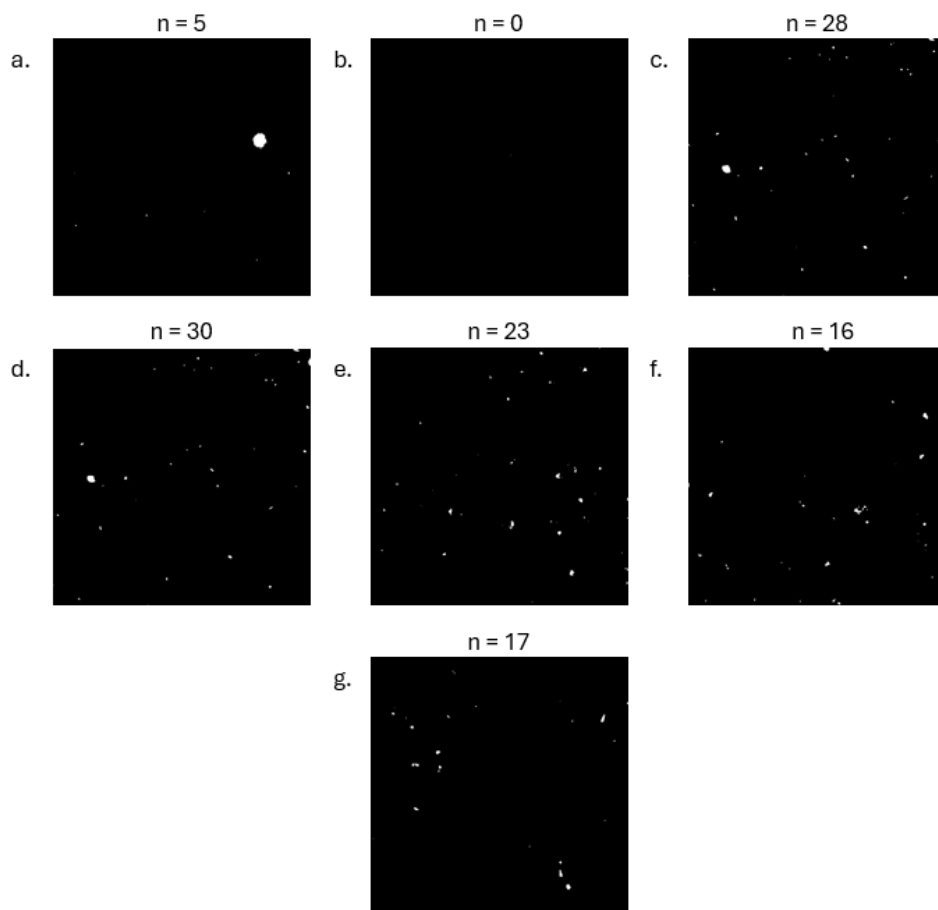
Figure 15. Microscope images of *S. enterica* on the surface of fluorinated silane modified PDMS, where n = number of bacteria. a) spot one showing 5 bacteria; b) spot two showing 0 bacteria; c) spot three showing 28 bacteria; d) spot four showing 30 bacteria; e) spot five showing 23 bacteria; f) spot six showing 16 bacteria; g) spot seven showing 17 bacteria. The MATLAB code in Appendix A was used to exclude particles based on size and shape.

P22 Bacteriophage. While the PDMS surface treated with P22 phage shows a very significant increase in the rate of bacterial adhesion, initially, the active phage on the surface will lyse the bacteria upon entrapment. This prohibits the bacteria from proliferating (or in a lysogenic state, proliferating viable cells). If the cells are unable to move or replicate, the chances of biofilm formation are likely decreased, showing potential for effective surface treatment. Figures 16a – g show that there are a total of 2,508 bacteria, with the most bacteria (with an accurate count) in one spot being 430 (Fig. 16b). Figures 16f and 16g were unable to get accurate bacterial counts, due to improper lighting. When setting the threshold for the image, before counting, the improper lighting does not allow many of the bacteria to be included in a usable threshold. The amounts for these are estimated using unprocessed images since bacterial resistance is not being observed for the phage surfaces.
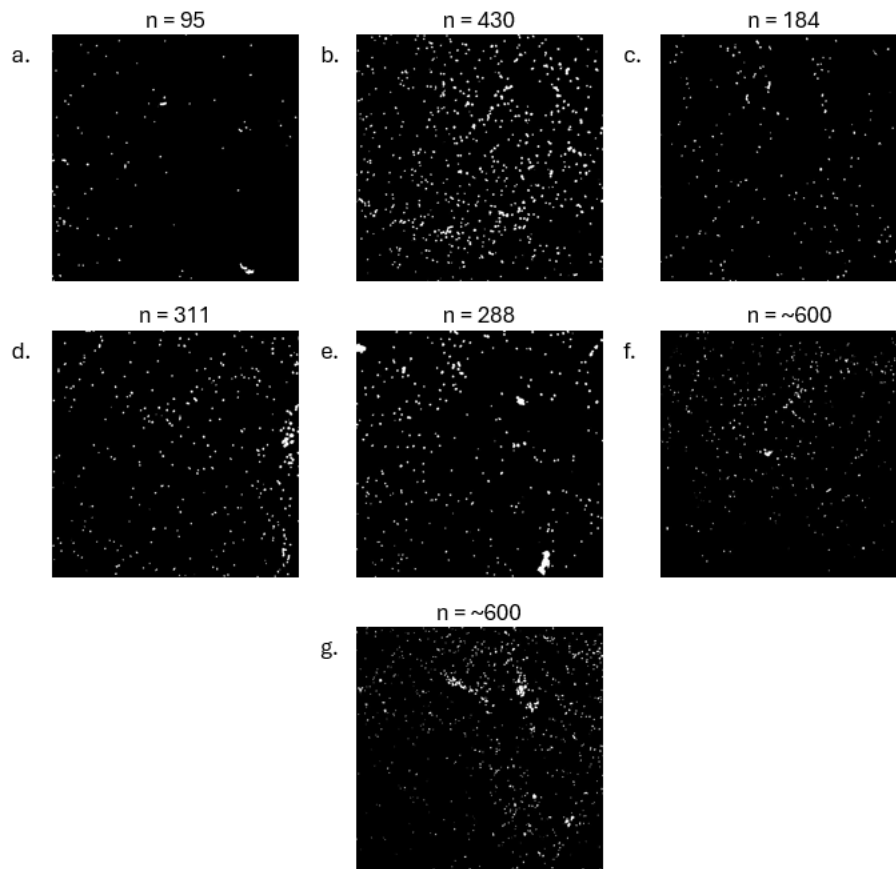
Figure 16. Microscope images of *S. enterica* on the surface of phage modified PDMS, where n = number of bacteria. a) spot one showing 95 bacteria; b) spot two showing 430 bacteria; c) spot three showing 184 bacteria; d) spot four showing 311 bacteria; e) spot five showing 288 bacteria; f) spot six showing ~ 600 bacteria; g) spot seven showing ~ 600 bacteria. The MATLAB code in Appendix A was used to exclude particles based on size and shape.

4. Conclusion

Initial results are presented from research that investigates bacterial adhesion, the first step in biofilm formation. It was found that the facile chemical treatment of a surface can inhibit adhesion of *S. enterica* microorganisms thereby reducing the potential for biofilm formation. This approach has wide applicability as the chemistry can be applied to virtually any substrate, such as metals and non-metals, including biocompatible materials. The hydrophobic surface of the fluorinated silane proved to be the most effective for resisting bacterial adhesion, and though, attachment of P22 bacteriophage increases the entrapment of *S. enterica* on a surface and we have shown the potential for the phage to destroy the microbial culture.

Future work will focus on the elucidation of the chemistry involved in adhesion of bacteria to surfaces. This would include the correlation between initial attachment, viewed in real time (within tens of minutes) under a microscope with long term colonization of surfaces (over several days). The work would include a determination of the viability of the bacteria once attached to a surface. While it is known that *Salmonella* will form biofilm under environmental stress, we did not observe the development of a biofilm under a variety of conditions. Understanding the mechanisms involved in the formation of biofilm is important in correctly interpreting our findings to ensure the relevance of the work. Of priority now is to investigate the adhesion of *Salmonella* to surfaces as a function of concentration, nutrition, flow rate, surface chemistry and topology. The successful outcome of this work will result in the development of new materials for medical applications, food packaging and food preparation.

5. References

Arnold, J. W., & Yates, I. E. (2009). Interventions for control of Salmonella: clearance of microbial growth from rubber picker fingers. *Poult Sci*, *88*(6), 1292-1298. https://doi.org/10.3382/ps.2008-00391

Bazaka, K., Jacob, M. V., Crawford, R. J., & Ivanova, E. P. (2012). Efficient surface modification of biomaterial to prevent biofilm formation and the attachment of microorganisms. *Appl Microbiol Biotechnol*, *95*(2), 299-311. https://doi.org/10.1007/s00253-012-4144-7

Bhunia, A. K. (2018). *Foodborne Microbial Pathogens : Mechanisms and Pathogenesis* (2nd 2018. ed.). Springer New York : Imprint: Springer. http://dx.doi.org/10.1007/978-1-4939-7349-1

Biederman, H. (2011). Nanocomposites and nanostructures based on plasma polymers. *Surface and Coatings Technology*, *205*, S10-S14. https://doi.org/https://doi.org/10.1016/j.surfcoat.2011.03.115

Bordi, C. d. B., S. . (2011). Hacking into bacterial biofilms: a new therapeutic challenge. *Ann. Intensive Care*, *1*(19). https://doi.org/https://doi.org/10.1186/2110-5820-1-19

Chiu, C. H., Wu, T. L., Su, L. H., Chu, C., Chia, J. H., Kuo, A. J., Chien, M. S., & Lin, T. Y. (2002). The emergence in Taiwan of fluoroquinolone resistance in Salmonella enterica serotype choleraesuis. *N Engl J Med*, *346*(6), 413-419. https://doi.org/10.1056/NEJMoa012261

Costerton, J. W., Stewart, P. S., & Greenberg, E. P. (1999). Bacterial biofilms: a common cause of persistent infections. *Science*, *284*(5418), 1318-1322. https://doi.org/10.1126/science.284.5418.1318

Decho, A. W. (2000). Microbial biofilms in intertidal systems: an overview. *Continental Shelf Research*, *20*(10-11), 1257-1273. https://doi.org/https://doi.org/10.1016/S0278-4343(00)00022-4

Eng, S. K., Pusparajah, P., Ab Mutalib, N. S., Ser, H. L., Chan, K. G., & Lee, L. H. (2015). Salmonella: A review on pathogenesis, epidemiology and antibiotic resistance. *Frontiers in Life Science*, *8*(3), 284-229. https://doi.org/https://doi.org/10.1080/21553769.2015.1051243

Galan, J. E. (1996). Molecular and cellular bases of Salmonella entry into host cells. *Curr Top Microbiol Immunol*, *209*, 43-60. https://doi.org/10.1007/978-3-642-85216-9_3

Galan, J. E., & Wolf-Watz, H. (2006). Protein delivery into eukaryotic cells by type III secretion machines. *Nature*, *444*(7119), 567-573. https://doi.org/10.1038/nature05272

Giaouris, E. D., & Nychas, G. J. (2006). The adherence of Salmonella Enteritidis PT4 to stainless steel: the importance of the air-liquid interface and nutrient availability. *Food Microbiol*, *23*(8), 747-752. https://doi.org/10.1016/j.fm.2006.02.006

Guerra, B., Soto, S., Helmuth, R., & Mendoza, M. C. (2002). Characterization of a self-transferable plasmid from Salmonella enterica serotype typhimurium clinical isolates carrying two integron-borne gene cassettes together with virulence and drug resistance genes. *Antimicrob Agents Chemother*, *46*(9), 2977-2981. https://doi.org/10.1128/AAC.46.9.2977-2981.2002

Guerra, B., Soto, S. M., Arguelles, J. M., & Mendoza, M. C. (2001). Multidrug resistance is mediated by large plasmids carrying a class 1 integron in the emergent Salmonella enterica serotype [4,5,12:i:-]. *Antimicrob Agents Chemother*, *45*(4), 1305-1308. https://doi.org/10.1128/AAC.45.4.1305-1308.2001

Hoffmann, S. (2015). Foodborne illnesses caused by Salmonella cost the U.S. an estimated $3.7 billion annually. In *USDA Economic Research Service*.

Homoe, P., Bjarnsholt, T., Wessman, M., Sorensen, H. C., & Johansen, H. K. (2009). Morphological evidence of biofilm formation in Greenlanders with chronic suppurative otitis media. *Eur Arch Otorhinolaryngol*, *266*(10), 1533-1538. https://doi.org/10.1007/s00405-009-0940-9

Hurrell, E., Kucerova, E., Loughlin, M., Caubilla-Barron, J., & Forsythe, S. J. (2009). Biofilm formation on enteral feeding tubes by Cronobacter sakazakii, Salmonella serovars and other Enterobacteriaceae. *Int J Food Microbiol*, *136*(2), 227-231. https://doi.org/10.1016/j.ijfoodmicro.2009.08.007

Joseph, B., Otta, S.K., Karunasagar, I. (2001). Biofilm formation by Salmonella spp. on food contact surfaces and their sensitivity to sanitizers. *International Journal of Food Microbiology*, *64*(3), 367-372. https://doi.org/https://doi.org/10.1016/S0168-1605(00)00466-9

Kasman, L. M., & Porter, L. D. (2024). Bacteriophages. In *StatPearls*. https://www.ncbi.nlm.nih.gov/pubmed/29630237

Lories, B., Roberfroid, S., Dieltjens, L., De Coster, D., Foster, K. R., & Steenackers, H. P. (2020). Biofilm Bacteria Use Stress Responses to Detect and Respond to Competitors. *Curr Biol*, *30*(7), 1231-1244 e1234. https://doi.org/10.1016/j.cub.2020.01.065

Ly, K. T., Casanova, J.E. . (2007). Mechanisms of Salmonella entry into host cells. *Cellular Microbiology*, *9*, 2103-2111. https://doi.org/https://doi.org/10.1111/j.1462-5822.2007.00992.x

Maillard, J. Y. (2005). Antimicrobial biocides in the healthcare environment: efficacy, usage, policies, and perceived problems. *Ther Clin Risk Manag*, *1*(4), 307-320. https://www.ncbi.nlm.nih.gov/pubmed/18360573

McGucken, P. V., & Woodside, W. (1973). Studies on the mode of action of glutaraldehyde on Escherichia coli. *J Appl Bacteriol*, *36*(3), 419-426. https://doi.org/10.1111/j.1365-2672.1973.tb04123.x

O'Hagan, D. (2008). Understanding organofluorine chemistry. An introduction to the C-F bond. *Chem Soc Rev*, *37*(2), 308-319. https://doi.org/10.1039/b711844a

Ohl, M. E., & Miller, S. I. (2001). Salmonella: a model for bacterial pathogenesis. *Annu Rev Med*, *52*, 259-274. https://doi.org/10.1146/annurev.med.52.1.259

Pakpour, N., & Horgan, S. (2021). Lab 9: Standard plate count. In *General Microbiology Lab Manual* https://bio.libretexts.org/Learning_Objects/Laboratory_Experiments/Microbiology_Labs/Book%3A_General_Microbiology_Lab_Manual_(Pakpour_and_Horgan)/Lab_09%3A_Standard_Plate_Count

Pistone, A., Scolaro, C., & Visco, A. (2021). Mechanical Properties of Protective Coatings against Marine Fouling: A Review. *Polymers (Basel)*, *13*(2). https://doi.org/10.3390/polym13020173

Prouty, A. M., & Gunn, J. S. (2003). Comparative analysis of Salmonella enterica serovar Typhimurium biofilm formation on gallstones and on glass. *Infect Immun*, *71*(12), 7154-7158. https://doi.org/10.1128/IAI.71.12.7154-7158.2003

Pui, C. F., Wong, W. C., Chai, L. C., Nillian, E., Ghazali, F. M., Cheah, Y. K., Nakaguchi, Y., Mitsuaki, N., & Radu, S. (2011). Simultaneous detection of Salmonella spp., Salmonella Typhi and Salmonella Typhimurium in sliced fruits using multiplex PCR. *Food Control*, *22*(2), 337-342.

Sardella, E., Favia, P., Gristina, R., Nardulli, M. and d'Agostino, R. . (2006). Plasma-Aided Micro- and Nanopatterning Processes for Biomedical Applications. *Plasma Processes Polym*, *3*, 456-469. https://doi.org/https://doi.org/10.1002/ppap.200600041

Sehmi, S. K., Allan, E., MacRobert, A. J., & Parkin, I. (2016). The bactericidal activity of glutaraldehyde-impregnated polyurethane. *Microbiologyopen*, *5*(5), 891-897. https://doi.org/10.1002/mbo3.378

Shea, J. E., Hensel, M., Gleeson, C., & Holden, D. W. (1996). Identification of a virulence locus encoding a second type III secretion system in Salmonella typhimurium. *Proc Natl Acad Sci U S A*, *93*(6), 2593-2597. https://doi.org/10.1073/pnas.93.6.2593

Stanton, M. M., Parrillo, A., Thomas, G. M., McGimpsey, W. G., Wen, Q., Bellin, R. M., Lambert, C. R. (2015). Fibroblast extracellular matrix and adhesion on microtextured

polydimethylsiloxane scaffolds. *Journal of biomedical materials research. Part B, Applied biomaterials*, *103*(4), 861-869. https://doi.org/https://doi.org/10.1002/jbm.b.33244

Steenackers, H., Hermans, K., Vanderleyden, J., De Keersmaecker, S. C. J. (2012). *Salmonella* biofilms: An overview on occurrence, structure, regulation and eradication. *Food Research International*, *45*(2), 502-531. https://doi.org/https://doi.org/10.1016/j.foodres.2011.01.038

Vander Byl, C., & Kropinski, A. M. (2000). Sequence of the genome of Salmonella bacteriophage P22. *J Bacteriol*, *182*(22), 6472-6481. https://doi.org/10.1128/JB.182.22.6472-6481.2000

Wang, C., Tu, J., Liu, J., & Molineux, I. J. (2019). Structural dynamics of bacteriophage P22 infection initiation revealed by cryo-electron tomography. *Nat Microbiol*, *4*(6), 1049-1056. https://doi.org/10.1038/s41564-019-0403-z

6. Appendices

Appendix A

MATLAB code used to detect bacteria in processed images, provided by Seyed Hamed Ghavami in part for this research:

```
clc,clear all; close all;

% Read the input image

[fnam, path] = uigetfile('*.jpg','Input image');


% Read the input image

inputImage = imread(fnam);


% Define parameters for bacteria detection

minBacteriaSize = 2;  % Minimum area for detected bacteria

maxBacteriaSize = 100; % Maximum area for detected bacteria

MaxCircularity= 0.9;


% Convert to grayscale and apply a threshold

grayImage = rgb2gray(inputImage);

binaryImage = imbinarize(grayImage, 'adaptive',Sensitivity=0.45);


% Find connected components (bacteria) in the binary image

CC = bwconncomp(binaryImage);


% Analyze properties of connected components

stats = regionprops(CC, 'Area', 'BoundingBox', 'Centroid','Eccentricity');


% Initialize a figure to display the results


figure;
```

```matlab
% subplot(1, 3, 1);

% imshow(inputImage);

subplot(1, 2, 1);

imshow(binaryImage);

subplot(1, 2, 2);

imshow(inputImage);

hold on;


% Initialize a counter for detected bacteria

detectedBacteriaCount = 0;


% Iterate through detected bacteria

for i = 1:length(stats)

    area = stats(i).Area;

    centroid = stats(i).Centroid;

    % Calculate circularity (circularity = 1 for perfect circles)

    circularity=stats(i).Eccentricity;

    % Filter bacteria based on size

    if area >= minBacteriaSize && area <= 4

        % Draw a bounding box around the detected bacteria

        % bbox = stats(i).BoundingBox;

        % rectangle('Position', bbox, 'EdgeColor', 'r', 'LineWidth', 2);

        % Mark the centroid

        plot(centroid(1), centroid(2), 'r+', 'MarkerSize', 8, 'LineWidth', 2);


        % Increment the detected bacteria count

        detectedBacteriaCount = detectedBacteriaCount + 1;

    end

    if area >= 5 && area <= 10  && circularity <= 0.98
```

```matlab
        % Draw a bounding box around the detected bacteria

        % bbox = stats(i).BoundingBox;

        % rectangle('Position', bbox, 'EdgeColor', 'r', 'LineWidth', 2);

        % Mark the centroid

        plot(centroid(1), centroid(2), 'r+', 'MarkerSize', 8, 'LineWidth', 2);


        % Increment the detected bacteria count

        detectedBacteriaCount = detectedBacteriaCount + 1;

    end

    if area > 10 && area <= maxBacteriaSize  && circularity <= MaxCircularity

        % Draw a bounding box around the detected bacteria

        % bbox = stats(i).BoundingBox;

        % rectangle('Position', bbox, 'EdgeColor', 'r', 'LineWidth', 2);

        % Mark the centroid

        plot(centroid(1), centroid(2), 'r+', 'MarkerSize', 8, 'LineWidth', 2);


        % Increment the detected bacteria count

        detectedBacteriaCount = detectedBacteriaCount + 1;

    end

end


hold off;

title(['Detected Bacteria: ', num2str(detectedBacteriaCount)]);


% save and display the result

saveas(gcf, ['result', fnam]);
```